

## Article

# 12-Vertex *closo*-3,1,2-Ruthenadecaboranes with Chelate POP-Ligands: Synthesis, X-ray Study and Electrochemical Properties

Anastasiya M. Zimina<sup>1</sup>, Nikolay V. Somov<sup>1</sup> , Yulia B. Malysheva<sup>1</sup>, Nadezhda A. Knyazeva<sup>1</sup>, Alexander V. Piskunov<sup>1,2</sup>  and Ivan D. Grishin<sup>1,\*</sup> 

<sup>1</sup> Lobachevsky State University of Nizhny Novgorod, 23 Gagarin Prosp., 603950 Nizhny Novgorod, Russia

<sup>2</sup> G.A. Razuvaev Institute of Organometallic Chemistry, Russian Academy of Sciences, 49 Tropinin Str., 603950 Nizhny Novgorod, Russia

\* Correspondence: grishin\_i@ichem.unn.ru

**Abstract:** A class of so-called POP ligands (Xantphos, NiXantphos, DPEphos) are of a great interest to the coordination chemistry due to their wide P-M-P bite angles and ability to show either  $\kappa^2$ - or  $\kappa^3$ -binding modes. Such  $\kappa^2$ - $\kappa^3$ -rearrangement is valuable for catalytic application and internal stabilization of intermediates. To widen the scope of ruthenium-based catalysts for Atom Transfer Radical Polymerization (ATRP) two new approaches to the synthesis of *closo*-ruthenadecaboranes with aforementioned POP ligands were developed and six new 17-e (3,3-(POP)-3-Cl-*closo*-3,1,2-RuC<sub>2</sub>B<sub>9</sub>H<sub>11</sub>; **2**, **4**, **7**) and 18-e (3,3-(POP)-3-NCCH<sub>3</sub>-*closo*-3,1,2-RuC<sub>2</sub>B<sub>9</sub>H<sub>11</sub>; **3**, **5**, **8**) clusters were synthesized and characterized by means of NMR or ESR spectroscopy, MALDI mass-spectrometry and single crystal X-ray diffraction studies. The unique 18-e complex of Ru(II) with dioxygen ligand 3,3-(DPEphos)-3-( $\eta^2$ -O<sub>2</sub>)-*closo*-3,1,2-RuC<sub>2</sub>B<sub>9</sub>H<sub>11</sub> (**9**) was isolated and characterized by X-ray diffraction. It was shown that aforementioned POP ligands coordinate to ruthenium by two phosphorus atoms in a  $\kappa^2$ -fashion. The performed electrochemical studies have shown reversible Ru(II)-Ru(III) transition making the complexes suitable for application in catalysis of polymerization. The test experiments on methyl methacrylate (MMA) polymerization indicate the proceeding of the process in according with an ATRP mechanism.

**Keywords:** ruthenadecaboranes; POP ligands; cyclic voltammetry; ATRP; X-ray; NMR



**Citation:** Zimina, A.M.; Somov, N.V.; Malysheva, Y.B.; Knyazeva, N.A.; Piskunov, A.V.; Grishin, I.D. 12-Vertex *closo*-3,1,2-Ruthenadecaboranes with Chelate POP-Ligands: Synthesis, X-ray Study and Electrochemical Properties. *Inorganics* **2022**, *10*, 206. <https://doi.org/10.3390/inorganics10110206>

Academic Editors: Marina Yu. Stogniy and Rainer Winter

Received: 13 October 2022

Accepted: 9 November 2022

Published: 11 November 2022

**Publisher's Note:** MDPI stays neutral with regard to jurisdictional claims in published maps and institutional affiliations.



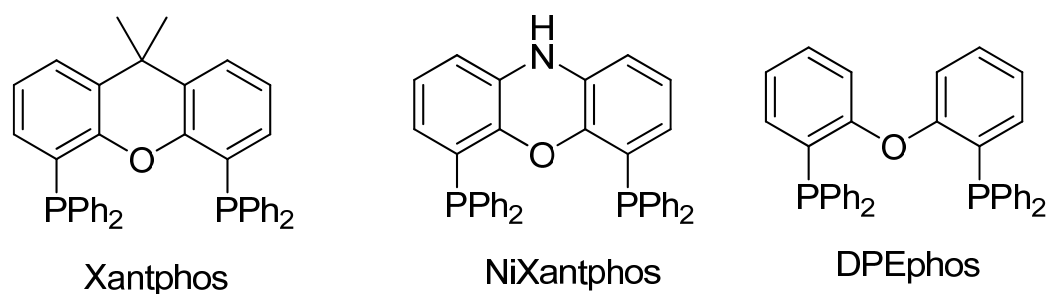
**Copyright:** © 2022 by the authors. Licensee MDPI, Basel, Switzerland. This article is an open access article distributed under the terms and conditions of the Creative Commons Attribution (CC BY) license (<https://creativecommons.org/licenses/by/4.0/>).

## 1. Introduction

Ruthenium complexes with chelate organodiphosphine ligands of the general formula 3,3-(P-P)-3-Cl-*closo*-3,1,2-RuC<sub>2</sub>B<sub>9</sub>H<sub>11</sub> (P-P = PPh<sub>2</sub>(CH<sub>2</sub>)<sub>n</sub>PPh<sub>2</sub>) are interesting compounds which have found application in catalysis of Atom Transfer Radical Polymerization (ATRP) process [1–3]. The analysis of recent publications shows that redox properties of the complex and its catalytic activity dramatically depend on the bite angle of the corresponding diphosphine ligand. The complexes with wide bite angles and flexible links between phosphorus atoms show better performance. Thus the change of diphosphine can be considered as a way of catalyst tuning. Among the known diphosphine ligands with large bite angles so-called POP ligands such as Xantphos, NiXantphos and DPEphos should be mentioned. A specific peculiarity of these ligands is the presence of oxygen atom which can act as an additional coordination site stabilizing ruthenium center. These ligands may be considered as hemilabile due to the ability to show either  $\kappa^2$ - or  $\kappa^3$ -binding modes. The latter peculiarity is of a special interest from the point of view of stabilization of transition 16-e species which are considered as intermediates in ATRP catalyzed by ruthenadecaboranes [2].

The reduction of the aforementioned 17-e Ru(III) *closo*-complexes by amines in acetonitrile media allows obtaining 18-e Ru(II) species of the general formula 3,3-(P-P)-3-NCCH<sub>3</sub>-

*closo*-3,1,2-RuC<sub>2</sub>B<sub>9</sub>H<sub>11</sub> [4,5]. The mechanism of its formation assumes the formation of 16-e intermediates further stabilized by acetonitrile molecule. Such species may be also stabilized by phosphine [6] or metal atom [7]. Another group of the known 18-e *closo*-ruthenacarboranes is represented by complexes with  $\kappa^3$ -triphosphine ligand. Coordination of the third phosphorus atom significantly increases the complex stability. Thus the dissociation of one arm of the ligand becomes unfavorable hampering its application in catalysis of polymerization processes. The use of hemilabile POP ligands seems a promising way to 18-e complexes capable to act as polymerization catalysts.



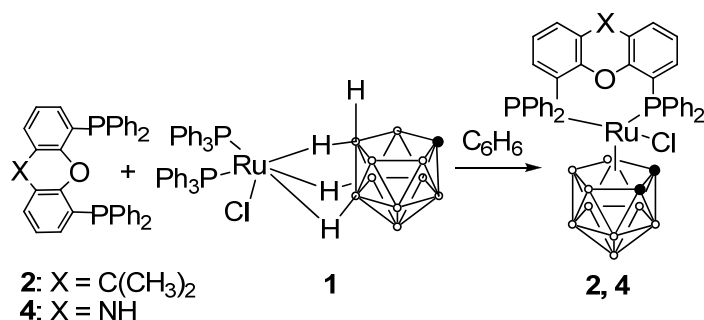
To evaluate the possibility of the formation of ruthenacarboranes containing aforementioned POP ligands, its influence on the electrochemical properties of the compounds and its ability to catalyze polymerization processes six novel complexes were synthesized and characterized by the means of X-ray study and cyclic voltammetry.

## 2. Results

### 2.1. Synthesis of Novel Ruthenacarboranes

A common way to produce ruthenacarboranes bearing chelate diphenylphosphine ligands with wide bite angles is the reaction of the corresponding RuCl<sub>2</sub>(PPh<sub>3</sub>)(diphosphine) with the salt of the *nido*-carborane [4]. The reaction of the known RuCl<sub>2</sub>(PPh<sub>3</sub>)(Xantphos) [8] with K<sup>+</sup>[*nido*-7,8-C<sub>2</sub>B<sub>9</sub>H<sub>12</sub>]<sup>−</sup> in benzene did not give the desired product neither at room temperature nor on heating. This fact may be explained by the action of Xantphos as a  $\kappa^3$ -ligand strongly occupying three equatorial sites in the ruthenium coordination sphere [9]. It makes the reaction with *nido*-carborane, which demands two vacant equatorial sites, impossible.

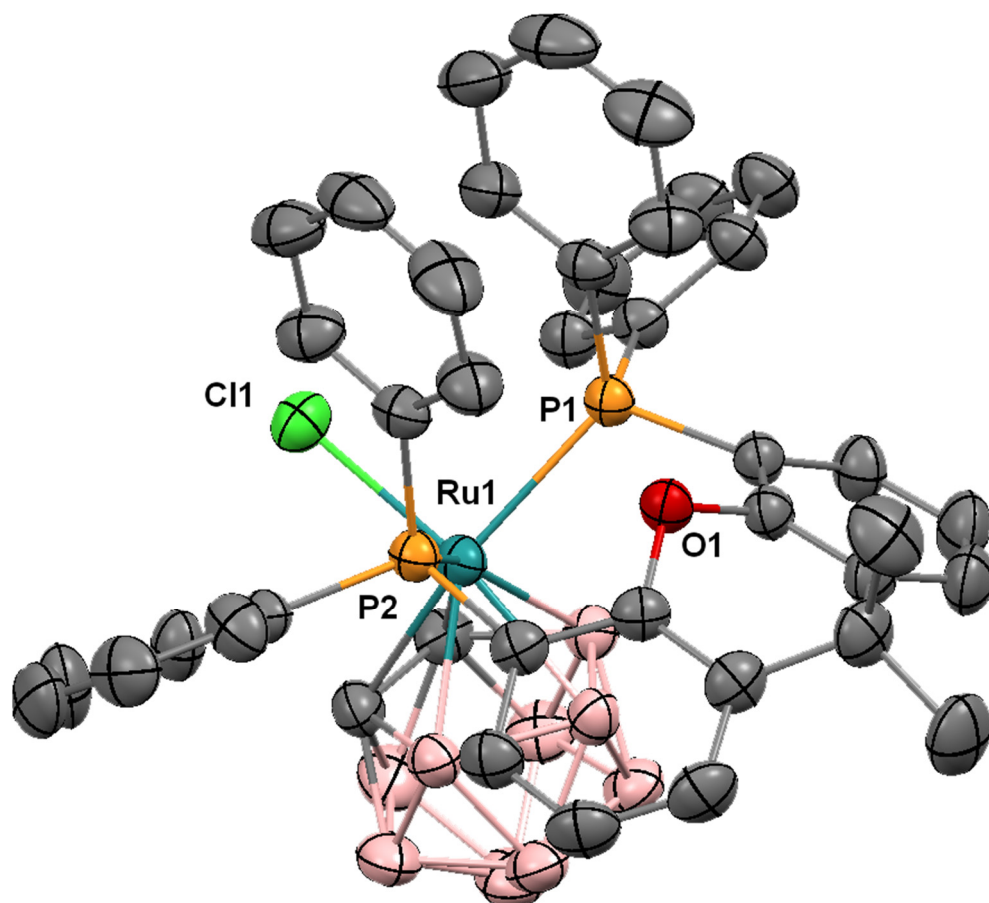
To obtain the targeted product an alternative approach starting from the known *exo-nido*-complex **1** was used. Heating **1** with Xantphos in benzene allowed us to synthesize novel *closo*-complex **2** (Scheme 1). It was isolated as dark-red crystals with 43.5% yield. According to the results of EPR study the complex is paramagnetic. Its anisotropic EPR spectrum (see Figure S1) is typical for *closo*-ruthenacarboranes with 17 electrons at metal center. The MALDI mass spectrum recorded in negative mode contains an envelope-type signal of molecular anion **2**<sup>−</sup> at *m/z* = 847.4 typical for such compounds [4,5].



**Scheme 1.** Synthesis of *closo*-ruthenacarboranes **2** and **4**.

The structure of **2** was finally determined by X-ray diffraction study and is represented at Figure 1 while the general structural parameters are provided in Table 1. Ruthenium

atom is coordinated to the opened  $C_2B_3$  plane of carborane ligand and bounded with chlorine ligand and two phosphorus atoms of Xantphos ligand. The oxygen atom of the ligand remains uncoordinated. A Ru–O distance is equal to 3.5388(13) Å and exceeds the sum of covalent radii. The mentioned distance is close to the same in the cyclopentadienyl-based ruthenium complexes with POP-ligands:  $RuCp^*XantphosCl$  (3.471 Å),  $RuCp^*XantphosH$  (3.500 Å) [10] or  $RuCpDPEphosCl$  (3.567 Å) [11]. At the same time this distance is longer than in the case of  $RuXantphos(CO)_2Cl_2$  (3.403 Å) [12] where Xantphos is also coordinated in a  $\kappa^2$ -fashion. The P–Ru–P bite angle (94.51 deg.) is close to the corresponding parameters of relative *closo*-ruthenacarboranes with long-chain diphosphines: 1,4-bis(diphenylphosphino)butane (92.06°) [13] and 1,5-bis(diphenylphosphino)pentane (94.42°) [14] and already mentioned complexes with POP ligands  $RuCp^*XantphosCl$  (94.14°),  $RuCp^*XantphosH$  (95.28°) and  $RuCpDPEphosCl$  (96.14°). At the same time it is significantly lower than in  $RuXantphos(CO)_2Cl_2$  (107.56°). Thus we may consider that the presence of a  $\eta^5$ -ligand in the molecules of **2** and Cp-based complexes leads to the increase of Ru–O distance and change of geometry of POP ligand. The C1–C2 bond (1.603 Å) and the distance between ruthenium atom and the center of  $C_2B_3$  plane (1.700 Å) in **2** are typical for *closo*-metallacarboranes [14–18].

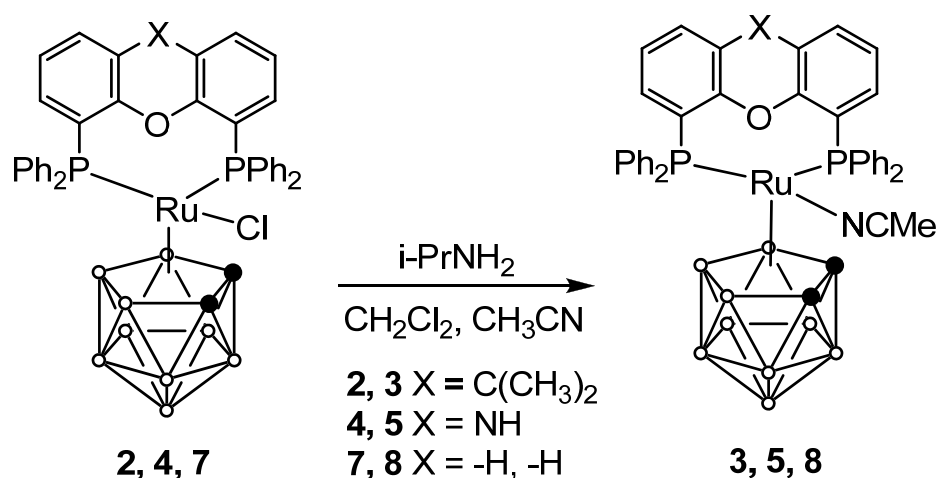


**Figure 1.** Molecular structure of ruthenacarborane **2** (thermal ellipsoids drawn at the 50% probability level). Hydrogen atoms have been omitted for clarity.

**Table 1.** Selected bond lengths (Å) and angles (deg.) in the discussed ruthenacarboranes.

Parameter	Compound			
	2	3	5	9
Bond lengths, Å				
Ru–P1	2.4016(6)	2.3606(6)	2.374(3)	2.3629(7)
Ru–P2	2.4048(6)	2.3666(6)	2.358(3)	2.3657(2)
Ru–Cl/N	2.3831(7)	2.064(2)	2.064(10)	-
Ru–O1	3.5388(17)	3.5028(16)	3.456(8)	3.6910(18)
Ru–O2	-	-	-	2.0399(18)
Ru–O3	-	-	-	2.0427(18)
Ru–C1	2.246(3)	2.206(2)	2.229(10)	2.286(2)
Ru–C2	2.248(3)	2.212(2)	2.209(12)	2.393(2)
Ru–B8	2.259(3)	2.293(3)	2.295(14)	2.278(3)
Ru–B7	2.248(3)	2.242(3)	2.258(13)	2.271(3)
Ru–B4	2.245(3)	2.243(3)	2.255(13)	2.271(3)
C1–C2	1.604(4)	1.631(3)	1.643(15)	1.595(4)
O2–O3	-	-	-	1.405(3)
Valence angles, deg.				
P1–Ru–P2	94.51(2)	95.58(2)	96.08(11)	92.47(2)
P1–Ru–Cl/N	91.65(2)	89.99(6)	91.9(3)	-
P2–Ru–Cl/N	92.47(2)	89.79(6)	88.4(3)	-

The reaction of complex **2** with isopropylamine in acetonitrile–methylene chloride mixture led to the corresponding complex **3** (Scheme 2). Diamagnetic nature of the complex allowed its investigation by the means of NMR spectroscopy. The  $^{31}\text{P}$  NMR spectrum of **3** is represented by a single line at 35.21 ppm showing the equivalence of phosphorus atoms due the rotation of carborane ligand.  $^1\text{H}$  NMR spectrum (Figure S2) is represented by the signals of protons of aromatic rings as multiplets at 6.73–7.62 ppm, the signal of  $\text{C}_{\text{carb}}\text{H}$  protons bounded to the carbons of carborane cage appears at 2.83 ppm. The methyl groups of acetonitrile and Xantphos ligands appear as sharp singlets at 2.47, 1.93 and 1.69 ppm. Different chemical shifts of methyl groups of Xantphos ligand indicate its unequivalence. The MALDI mass spectrum of **3** recorded in positive mode is has a signal at 812.3 Da corresponding to a  $[\text{3-CH}_3\text{CN}]^+$  cation formed through the dissociation of acetonitrile molecule. The similar signals were earlier observed for similar *closo*-ruthenacarboranes containing diphosphine and nitrile ligands.

**Scheme 2.** Synthesis of 18-e complexes **3**, **5** and **8**.

The performed X-ray analysis has confirmed the *closo*-structure of the complex and incorporation of acetonitrile molecule into its structure (Figure 2). The Ru–N distance

(2.064(2)Å) is typical for 18-e *closo*-ruthenacarboranes with nitrile ligands [4–6]. The structure of complex **3** provided on Figure 2 clearly shows that Xantphos ligand is symmetrically coordinated to the ruthenium atom in a  $\kappa^2$ -fashion. The lengths of Ru–P bonds and Ru–O distance are similar to the same in complex **2**. Thus, the spectral and structural data unambiguously show that in spite of the presence of oxygen atom, Xantphos acts a  $\kappa^2$ -ligand. Additional acetonitrile molecule is required to form stable 18-e complexes. The analysis of structural data shows that  $\kappa^3$ -coordinated Xantphos requires three equatorial coordination sites [9]. In the case of the formation of hypothetical 18-e *closo*-ruthenacarborane with  $\kappa^3$ -coordinated Xantphos the latter should occupy two equatorial and one axial coordination sites, but it is impossible due to the rigid structure of the ligand.

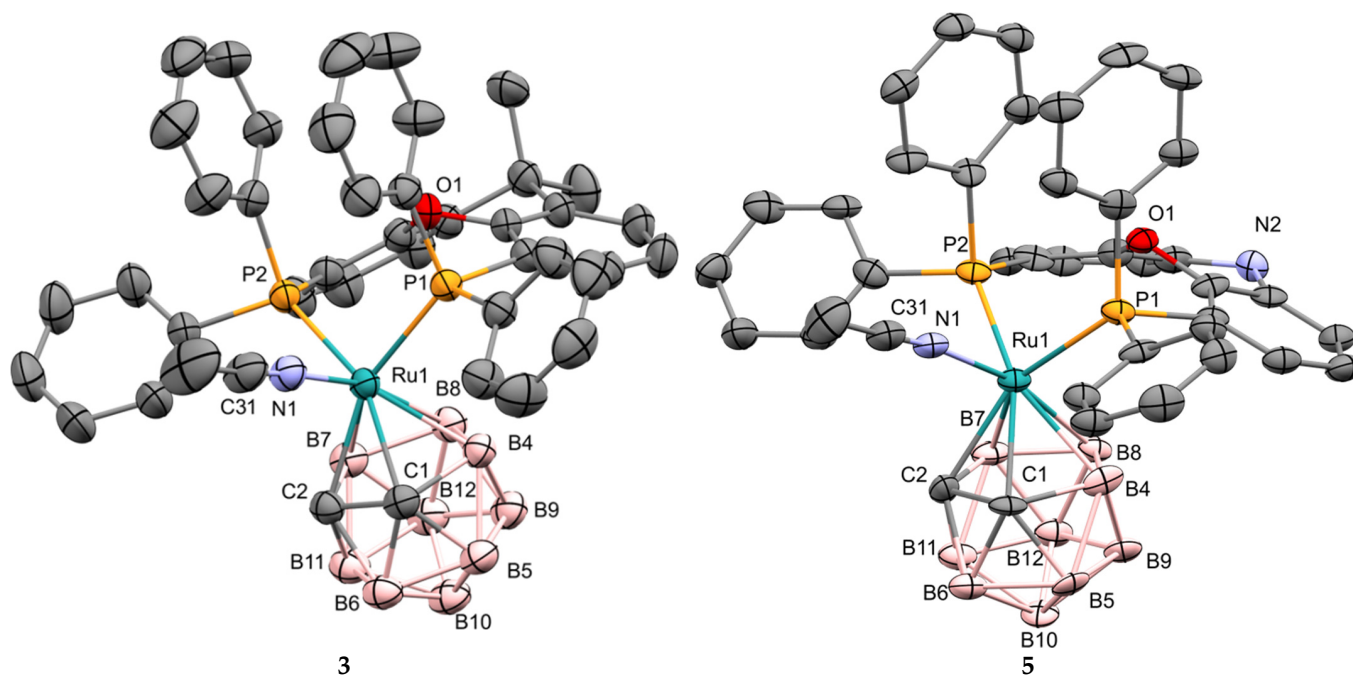
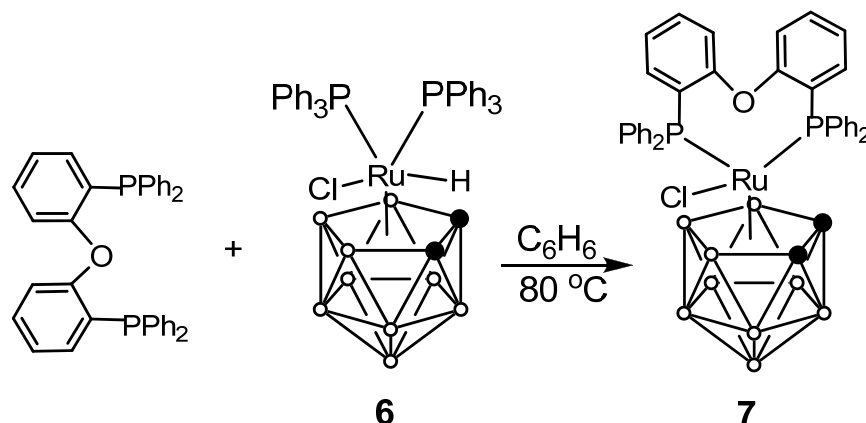


**Figure 2.** Molecular structures of ruthenacarboranes **3** and **5** (thermal ellipsoids drawn at the 50% probability level). Hydrogen atoms have been omitted for clarity.

Reaction of complex **1** with NiXantphos, a close analogue of Xantphos, resulted in formation of novel complex **4** with 40% yield (Scheme 1). The anisotropic ESR spectrum of **4** with  $g_1 = 2.524$ ;  $g_2 = 2.043$ ;  $g_3 = 1.937$  (Figure S1) is similar to the same of **2** being typical for *closo*-ruthenacarboranes. The presence of strong signal at 821.2 Da in MALDI mass spectrum recorded in negative mode confirms the proposed structure. Further reduction of **4** by isopropylamine (Scheme 2) allowed to isolate 18-e diamagnetic complex **5** being a close analogue of **3**. Its structure was confirmed by  $^{31}\text{P}$  and  $^1\text{H}$  MNR spectra and X-ray study.  $^{31}\text{P}$  NMR spectrum is represented by one signal from equivalent phosphorus atoms at 29.25 ppm while the  $^1\text{H}$  NMR (Figure S4) spectrum contains signals of aromatic rings (6.6–7.6 ppm),  $\text{C}_{\text{carb}}\text{H}$  protons of the cage (2.98 ppm), and a singlet from methyl group of acetonitrile (1.97 ppm)

As expected the structure of **5** represented on Figure 2 is very similar to the same of **3** and is characterized by the close values of bond lengths and valence angles (Table 1). NiXantphos also acts as a  $\kappa^2$ -ligand, no coordination of oxygen to ruthenium is observed. The structure of **5** was determined by X-ray diffraction. According to the CCDC database the complex is the first ruthenium compound containing a NiXantphos ligand. The P–Ru–P bite angle in **5** (96.08 deg.) is close to the same in complex **4** (95.58 deg.) but significantly lower than in rhodium-based complex NiXantphosRh(CO)HPPPh<sub>3</sub> (110,21°) [19] with  $\kappa^2$ -bounded POP ligand.

The attempt to obtain the analogue of **2** and **4** with more flexible DPEphos ligand by the aforementioned way (Scheme 1) was unsuccessful. To overcome this difficulty an alternative approach starting from *closo*-complex **6** was proposed (Scheme 3).

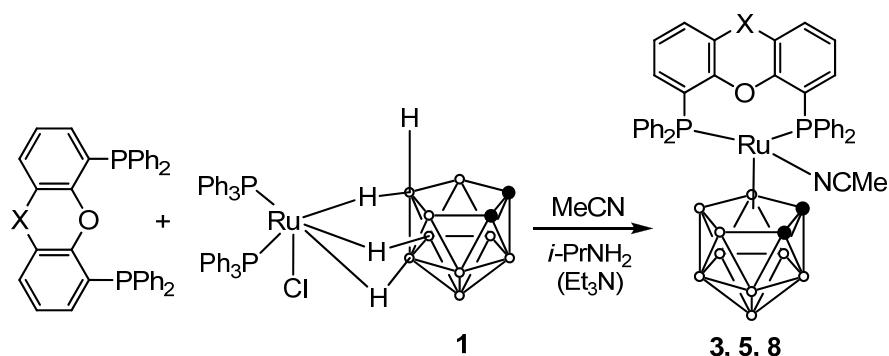


**Scheme 3.** Synthesis of DPEphos-based *closo*-ruthenacarborane **7**.

The reaction performed in benzene at 80 °C allowed to isolate compound **7** as dark-red crystals with 52% yield. The paramagnetic nature of the complex was confirmed by registration of its anisotropic EPR spectrum with  $g_1 = 2.433$ ;  $g_2 = 2.068$ ;  $g_3 = 1.955$  (Figure S1). MALDI mass spectrum is represented by an envelope-type signal at  $m/z = 806.0$  Da typical for ruthenacarboranes which confirms the formation of the complex.

Reduction of complex **7** by isopropylamine (Scheme 2) prospectively led to the formation of the complex **8** containing acetonitrile molecule with 80% yield. The structure of complex **8** was confirmed by the means of  $^1\text{H}$  NMR spectroscopy. The  $^{31}\text{P}$  NMR spectrum contains one signal from equivalent phosphorus atoms at 24.83 ppm. The  $^1\text{H}$  NMR spectrum (Figure S5) contains the signals of aromatic rings in the range 6.8–7.4 ppm, signals of  $\text{C}_{\text{carb}}\text{H}$  protons at 2.43 ppm and acetonitrile ligand at 1.99 ppm. The introduction of acetonitrile ligand in the complex was confirmed by the presence of a band at  $2253\text{ cm}^{-1}$  in the IR spectrum recorded in a solid matrix of KBr. Thus the introduction of acetonitrile molecule in the complex confirmed by NMR and IR spectra allows us to propose that DPEphos also acts a  $\kappa^2$ -ligand.

Further experiments have shown that 18-e complexes **3**, **5** and **8** may be directly obtained from *exo-nido*-complex **1** by its one-pot reaction with corresponding diphosphine and isopropylamine in acetonitrile media (Scheme 4) [4]. Conducting this reaction allows significant increasing of the total yield of the complexes up to 60–90% and decreasing the number of stages. It should be noted that in the case of complex **8** the use of triethylamine was more rational as allows increasing the yield up to 92%. The products formed by the reaction depicted on Scheme 4 have similar NMR, IR and MALDI MS spectra to those obtained in reactions on Scheme 2.



**Scheme 4.** An alternative route to *closo*-ruthenacarboranes **3**, **5** and **8**.

## 2.2. Electrochemical Studies

Electrochemical behavior of the obtained complexes was investigated by the means of cyclic voltammetry. The electrochemical experiments were provided using Ag|Ag<sup>+</sup> pseudo reference electrode, however the values of potentials were referred to ferrocene as internal standard to provide more particular comparison with the earlier published results. The recorded CVA curves are provided on Figure 3 while the calculated values of redox potentials are summarized in Table 2.

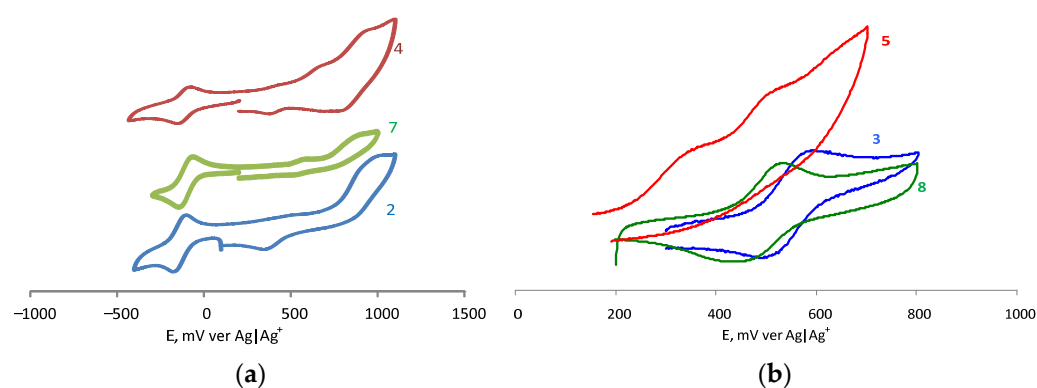


**Figure 3.** CVA curves recorded for (a) 17-e complexes 2, 4, 7; (b) 18-e complexes 3, 5, 8.

**Table 2.** The results of electrochemical studies of the obtained ruthenacarboranes <sup>1</sup>.

Transition	Compound						
	2	4	7	3	5	8	
M <sup>-</sup> /M	E <sub>pa</sub> , mV	-298	-280	-274	-	-	-
	E <sub>pc</sub> , mV	-369	-360	-350	-	-	-
	E <sub>1/2</sub> , mV	-333	-320	-312	-	-	-
	E <sub>pa</sub> - E <sub>pc</sub> , mV	71	80	76	-	-	-
M/M <sup>+</sup>	E <sub>pa</sub> , mV	800	471 <sup>2</sup>	702	331	360 <sup>3</sup>	395
	E <sub>pc</sub> , mV	-	-	-	242	-	300
	E <sub>1/2</sub> , mV	-	-	-	286	-	348
	E <sub>pa</sub> - E <sub>pc</sub> , mV	-	-	-	94	-	94

<sup>1</sup> The values are referred to ferrocene; <sup>2</sup> E<sub>pa</sub> = 741 mV for the second wave; <sup>3</sup> E<sub>pa</sub> = 510 mV for the second wave.

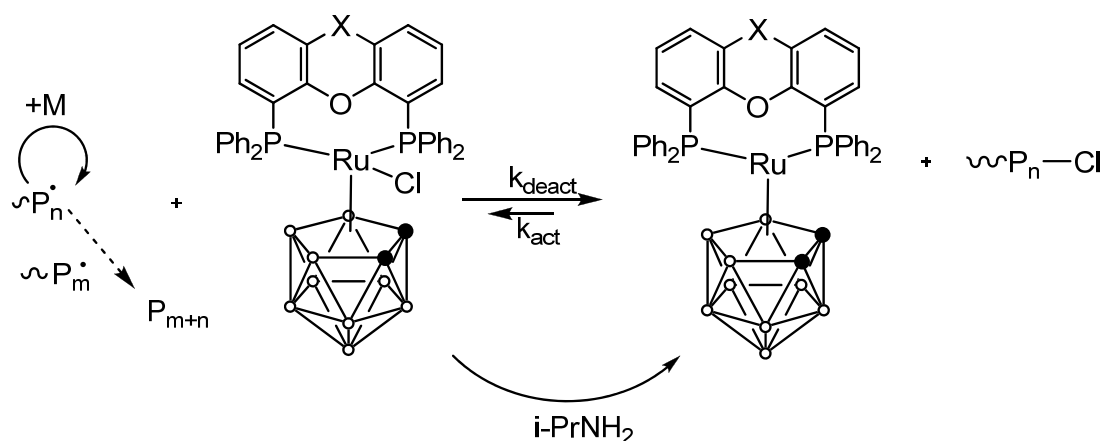
The performed experiments shown that 17-e paramagnetic complexes undergo reversible reduction to corresponding 18-e Ru(II) anions. The E<sub>1/2</sub> values for reduction process lie in the range -310–(-335) mV versus ferrocene and are close to those of *closo*-ruthenacarboranes with chelate bis(diphenylphosphino)alkanes [4–6]. Xanthphos-based complex 2 has the lowest redox potential while the highest one is observed for its DPEphos counterpart. The differences in potentials of anodic and cathodic peaks are about 70–80 mV being typical for reversible one-electron process. Oxidation of 17-e complexes proceeds fully irreversibly. Among the studied compounds complex 4 with NiXantphos ligand is oxidized at the lowest potential. Its oxidation is characterized by two consecutive waves which can be attributed to the step-by-step oxidation of NH fragment. According to the obtained data, complex 2 with Xantphos is the most stable towards oxidation.

Complexes 3 and 8 are characterized by redox transitions at 286 and 348 mV versus ferrocene respectively. Oxidation of these compounds to Ru(III) species proceeds pseudoreversible. The difference between potentials corresponding to anodic and cathodic peaks is about 90 mV. A Xantphos-based complex 3 has lower potential of oxidation in comparison with its DPEphos analogue. Oxidation of complex 5 containing NiXantphos ligand is fully irreversible and is also characterized by the presence of two consecutive waves which can be assigned to the oxidation of the ligand as in the case of 4.

The results of the performed electrochemical studies show that novel ruthenacarboranes with POP ligands generally similar to the earlier studied compounds based on bis(diphenylphosphino)alkanes [3–6], thus they should be capable to catalyze polymerization via ATRP mechanism. According to the measured values of potentials, Xantphos-based complexes seem to be the most prospective catalysts.

### 2.3. Catalysis of Radical Polymerization

As was mentioned in the introduction, some *closo*-ruthenacarboranes are capable of acting as catalysts of controlled radical polymerization via ATRP mechanism. To evaluate the possibility of application of the novel complexes as catalysts the tests experiments on methyl methacrylate (MMA) polymerization were performed. The polymerization was conducted in the presence of carbon tetrachloride as initiator. Isopropylamine was added as a reducing agent in accordance with Activators Generated by Electron Transfer (AGET) ATRP concept (Scheme 5) [3]. For precise dosage of initiator and decreasing the viscosity of the media toluene was added. The results of experiments on polymerization are provided in Table 3.



**Scheme 5.** The proposed mechanism of AGET ATRP catalyzed by ruthenacarboranes.

**Table 3.** The results of experiments on MMA polymerization in the presence of novel ruthenacarboranes at 80 °C. [MMA]: [CCl<sub>4</sub>]: [Ru]: [i-PrNH<sub>2</sub>] = 10,000: 25: 1: 40. Polymerization time—160 min.

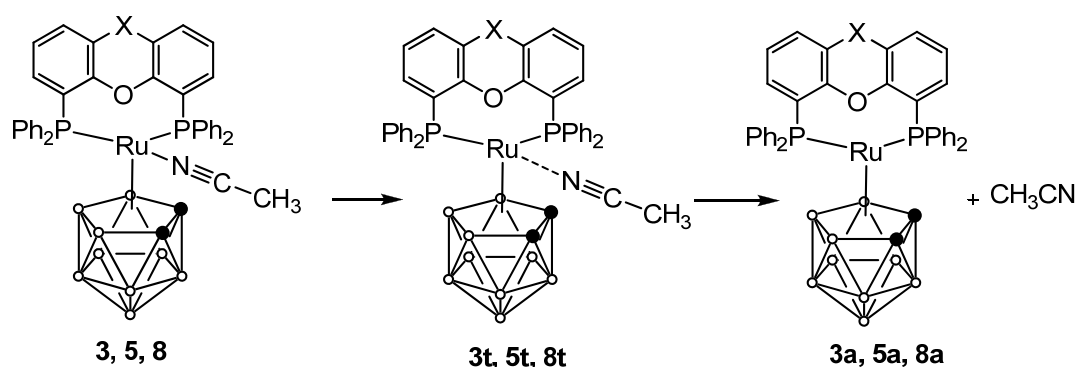
Complex	Type	Conversion	$M_n \times 10^{-3}$	$M_w/M_n$	$M_{n,theor} \times 10^{-3}$
2	17-e	61	21.4	1.5	24.4
3	18-e	94	27.2	1.6	37.6
4	17-e	70	23.5	1.7	28.0
5	18-e	68	25.5	1.8	27.2
7	17-e	68	52.6	2.2	27.2
8	18-e	75	59.3	2.4	30.0

The results of experiments of polymerization show that the obtained complexes are capable of catalyzing polymerization of MMA initiated by carbon tetrachloride. The highest monomer conversion for the set time was observed in the presence of 18-e complexes of Ru(II) **3** and **8**. The use of its chlorine-containing 17-e species resulted in the decrease of monomer conversion, but allowed to obtain polymers with more narrow molecular weight distribution. The lowest dispersity was observed for samples obtained in the presence of Xantphos-based complex **2**. The molecular weights agree with theoretically calculated values indicating a high degree of control over the process. The use of its NiXantphos analogue **4** led to the slight increase of polymer yield but resulted in increase of molecular weight distribution. The later may be caused by the worse oxidation stability of the complex and possible side reactions caused by the presence of NH fragment reactive to free radicals.

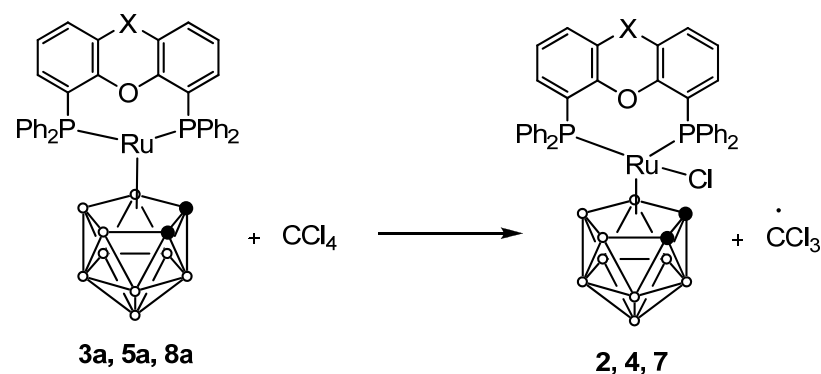
The use of DPEphos-based complexes **7** and **8** surprisingly led to the polymers with high dispersities and molecular weights significantly exceeding the theoretically calculated ones. The loss of the control over the process in comparison with Xantphos based complexes may be caused by lower electron density observed in electrochemical measurements or by higher flexibility of the ligand creating additional steric hindrances.

#### 2.4. DFT Studies of the Complexes

To estimate the influence of electronic and steric factors on the catalytic performance of the complexes quantum-chemical calculations were provided. We have calculated the energies of dissociation of acetonitrile ligand from complexes **3**, **5**, **8** leading to corresponding 16-e species **3a**, **5a**, **8a** (Scheme 6, I). The geometries of transition states **3t**, **5t**, **8t** for ligand dissociation reaction were also optimized. The energy changes in the chlorine transfer reaction between mentioned 16-e species and carbon tetrachloride used as an initiator of polymerization (Scheme 7, II) were also estimated using DFT. The results are summarized in Table 4.



Scheme 6. The mechanism of acetonitrile ligand dissociation.



Scheme 7. Reaction of 16-e species with CCl<sub>4</sub>.

Table 4. The calculated energy changes for the reactions depicted on Scheme 6 (I) and Scheme 7 (II).

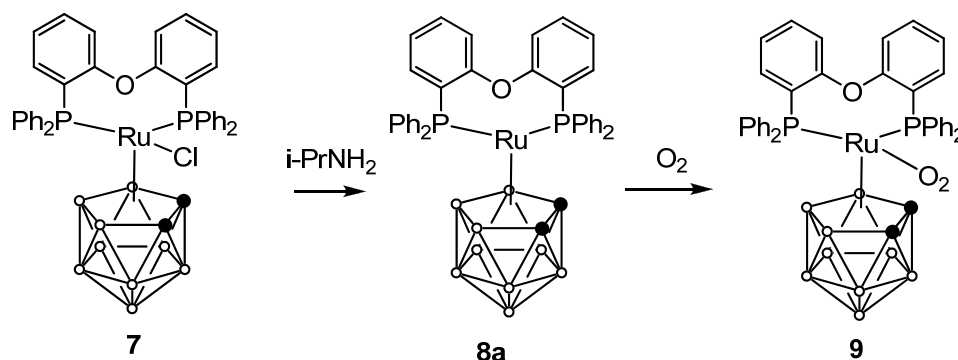
Ligand	Energy Change in Reaction, kcal/mol						
	I				II		
	$\Delta_r E$	$\Delta_r H$	$\Delta_r G$	E(TS)	$\Delta_r E$	$\Delta_r H$	$\Delta_r G$
Xantphos	14.1	14.1	2.6	13.7	1.8	2.2	1.6
NiXantphos	14.6	14.6	3.1	14.0	1.0	1.4	1.0
DPEphos	8.9	8.7	−1.9	15.1	15.1	15.8	13.1

The results of the performed calculations indicate that the energies of acetonitrile dissociation in the case of Xantphos and NiXantphos-based complexes are close to each

other and to the corresponding complex of 1,4-bis(diphenylphosphino)butane [6]. At the same time in the case of DPEphos dissociation of acetonitrile ligand requires lower energy. This fact may be explained by the possible internal stabilization of 16-e species with oxygen atom of flexible DPEphos ligand. Ru–O distance in the optimized structure of **8a** is equal to 2.434 Å. This distance is rather high to be considered as a covalent R–O bond but is significantly shorter than corresponding distances in **3a** (3.297 Å) and **5a** (3.240 Å). At the same time the energies of transition states for dissociation reaction are quiet similar for all three acetonitrile complexes and are about 13–14 kcal/mol. This energy is close to the energy of ligand dissociation in complexes **3** and **5** but higher than in case of **8**. The performed calculations indicate the possibility of internal stabilization of **8a** due to the coordination with oxygen atom of DPEphos ligand. The higher stability of **8a** results in increase the energy change for reaction depicted on Scheme 7 in comparison with complexes **3a** and **5a**. It should result in decrease of initiation ability in controlled radical polymerization and agrees with the poor control of the process discussed earlier.

### 2.5. The Studies of Transformations of DPEphos-Based Complexes

The predicted relative stability of complex **8a** inspired our attempts to isolate it in a pure form. According to the earlier published data [6] complex **8a** may be considered as an intermediate in the reaction of **7** with isopropylamine (Scheme 3). Conducting the reaction between **7** and amine in non-coordinative solvent should give the corresponding species (Scheme 8).



**Scheme 8.** The proposed mechanism of formation of *closo*-ruthenacarborane **9**.

The interaction of **7** with isopropylamine in benzene at room temperature resulted in quick change of solution color from red to yellow. Conducting this reaction in argon-flushed NMR tube has clearly shown the formation of novel diamagnetic species from initial 17-e paramagnetic complex **7**. Figure 4 represents the  $^{31}\text{P}$  NMR spectra just after reaction and after 24 h. The first spectrum is represented by two singlets at 22.64 and 23.13 ppm. The chemical shifts are close to the value of 24.83 ppm observed for complex **8**. The storage of the solution at room temperature led to the increase of the intensity of a downfield signal and appearance of a new signal at  $-17.51$  ppm relating to the free DPEphos ligand due to the partial decomposition of **8a**. The exchange of isopropylamine by triethylamine has no influence on the chemical shifts of the peaks, but results in the change of its relative intensities (Figure 4c). The similarity of the spectra obtained in the presence of different amines indicates that these amines should not be considered as auxiliary ligands forming 18-e complexes. The most intensive signal is probably assigned to complex **8a**, while the downfield signal may be assigned to the corresponding oxygen containing complex **9** which may be formed by a reaction of **8a** with traces of oxygen. The increase of the content of **9** with time is in a full agreement with this proposition.

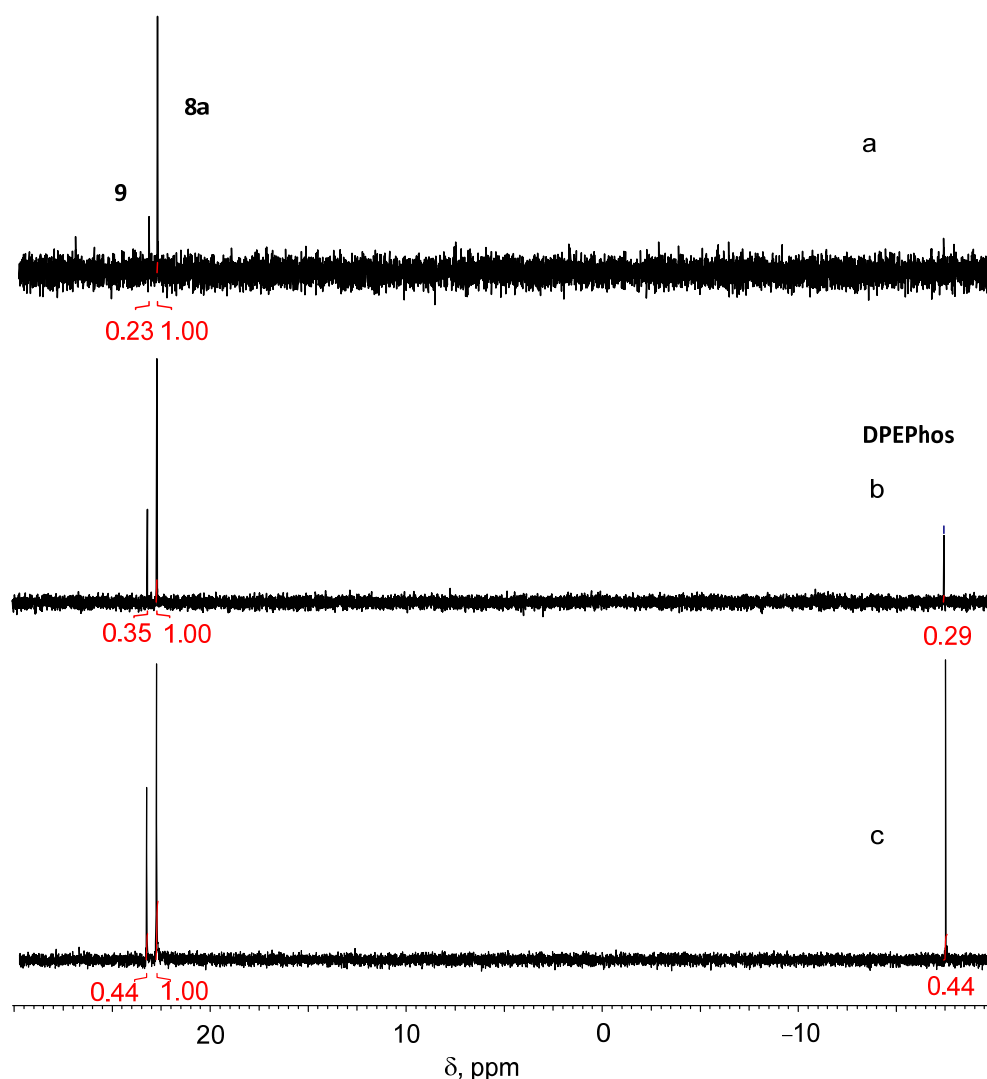


**Figure 4.**  $^{31}\text{P}$  NMR spectra recorded for the reaction of complex **7** with isopropylamine just after mixing (a) and after 24 h (b) or trimethylamine (c).

The attempts to isolate the products of reaction of complex **7** with isopropylamine by column separation and recrystallization from chloride—*n*-hexane mixture yielded some maroon crystals suitable for the X-ray diffraction study. The performed analysis confirmed the formation of the proposed oxygen-containing complex **9**. Its structure is depicted on Figure 5 while the main geometrical parameters provided in Table 1.

According to the results of X-ray study, complex **9** is a *closo*-ruthenacarborane containing chelate DPEphos ligand and an oxygen molecule as a  $\eta^2$ -ligand. The  $\text{O}_2$ – $\text{O}_3$  distance (1.405(3) Å) is close to the same in the previously obtained ruthenacarboranes [3-( $\eta^2$ - $\text{O}_2$ )-3,3,8-[ $\text{Ph}_2\text{P}(\text{CH}_2)_n\text{PPh}-\mu$ -( $\text{C}_6\text{H}_4$ -*ortho*)]-1,2- $\text{Me}_2$ -*closo*-3,1,2- $\text{RuC}_2\text{B}_9\text{H}_8$ ] ( $n = 3, 4$ ; 1.399(4), 1.404(4) Å) obtained in the Chizhevsky's group [20] and the similar  $\text{Cp}^*$ -based complexes such as [ $\text{Cp}^*\text{Ru}(\text{O}_2)(\text{dppe})$ ] $\text{PF}_6$  (1.398(5)) Å [21]). This distance is longer than in the free  $\text{O}_2$  molecule indicating the  $\eta^2$ -coordination by the  $\pi$ -bond. The ruthenium atom is symmetrically coordinated with dioxygen ligand with Ru–O distances 2.0399(18) and 2.0427(18) Å. The Ru–P bonds are also equal 2.3629(7)–2.3657(2) Å and have similar lengths to the same in Ru(II) complexes **3** and **5** and shorter than the corresponding bonds in Ru(III) complex **2** (see Table 1). The discussed bond lengths and the diamagnetic nature of complex **9** allows to consider it as a Ru(II) compound. It should be noted that in spite of the ruthenacarboranes with dioxygen ligand were already known, complex **9** is the first example of such type of compounds based on unsubstituted [ $\text{C}_2\text{B}_9\text{H}_{11}$ ] $^{2-}$  ligand.

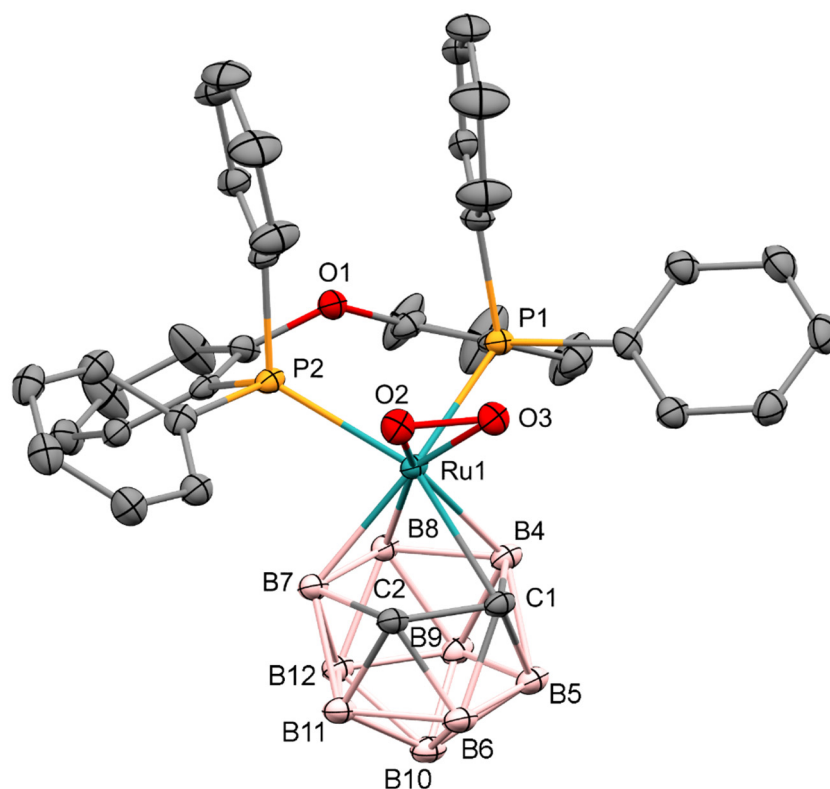


**Figure 5.** Molecular structure of ruthenacarborane **9** (thermal ellipsoids drawn at the 50% probability level). Hydrogen atoms have been omitted for clarity.

### 3. Materials and Methods

#### 3.1. General Considerations

All reactions were carried out under an argon atmosphere. Benzene (b.p. 80 °C) and toluene (b.p. 110 °C) were purified by distillation over sodium under an argon atmosphere. *n*-Hexane (b.p. 68 °C), methylene chloride (b.p. 40 °C), carbon tetrachloride (b.p. 77 °C) and acetonitrile (b.p. 82 °C) were distilled over calcium hydride. 4,5-Bis(diphenylphosphino)-9,9-dimethylxanthene (Xantphos), 4,6-Bis(diphenylphosphino)-10*H*-phenoxazine (NiXantphos) and Bis[(2-diphenylphosphino)phenyl] ether (DPEphos) were obtained from Dalchem (Russia) and stored under an argon atmosphere. Isolation of the products by column chromatography and its recrystallization was carried under argon flush. Column chromatography was performed on silica gel (230–400 mesh) from Macherey-Nagel. <sup>1</sup>H, <sup>31</sup>P and <sup>11</sup>B NMR spectra were obtained on Agilent DD2 NMR 400NB instrument. The EPR spectra were recorded in frozen toluene/CH<sub>2</sub>Cl<sub>2</sub> (1:1) mixture at 150 K with a Bruker-EMX spectrometer, operating at 9.75 GHz. IR spectra were recorded using Infracum FT spectrometer. MALDI-TOF mass-spectra of complexes were obtained in a linear mode using a Bruker Microflex LT system and *trans*-2-[3-(4-*tert*-butylphenyl)-2-methyl-2-propenylidene] malononitrile (DCTB) as a matrix. The solutions were applied to a stainless steel target plate according to a known method]. Polymerization of MMA was performed in glass tubes under a residual pressure of monomer (1.3 Pa) in the presence of 25 vol. % of toluene [2]. The MWDs of the polymer samples were determined by SEC in THF. Complexes *exo*-5,6,10-[Cl(PH<sub>3</sub>)<sub>2</sub>Ru]-5,6,10-(μ-H)<sub>3</sub>-10-*H-nido*-7,8-C<sub>2</sub>B<sub>9</sub>H<sub>8</sub> (**1**) and 3,3-(PPh<sub>3</sub>)<sub>2</sub>-3-*H*-3-*Cl-closo*-3,1,2-RuC<sub>2</sub>B<sub>9</sub>H<sub>11</sub> (**6**) were obtained in accordance with the previously described methods [22,23].

#### 3.2. Synthesis of Novel Ruthenacarboranes

[3,3- $\kappa^2$ -Xantphos-3-*Cl-closo*-3,1,2-RuC<sub>2</sub>B<sub>9</sub>H<sub>11</sub>] (**2**) Complex **1** (110 mg, 0.138 mmol) and Xantphos (87 mg, 0.151 mmol) were placed in a Schenk flask and degassed via three

vacuum–argon cycles and 15 mL of freshly distilled benzene were added in argon flow. The reaction was carried under argon atmosphere at 80 °C with stirring for 3 h. The solution was concentrated under vacuum and the residue was placed on a silica-gel filled column. The first dark red band was eluted by benzene. The solution was evaporated, and residue was recrystallized from benzene/n-hexane to give 50.8 mg (43.5%) of complex **2**. ESR (toluene-CH<sub>2</sub>Cl<sub>2</sub>, 150 K):  $g_1 = 2.502$ ,  $g_2 = 2.049$ ,  $g_3 = 1.942$ ; IR (KBr): 2574 cm<sup>-1</sup> ( $\nu$ (B-H)). MALDI MS ( $M^-$ , max): 847.4 ( $M^-$ ; isotopic pattern for 1Ru, 1Cl, 9B atoms), calcd.: 847.2.

[3,3- $\kappa^2$ -NiXantphos-3-Cl-closo-3,1,2-RuC<sub>2</sub>B<sub>9</sub>H<sub>11</sub>] (**4**) The procedure is similar as for the complex **2**. Heating of 130 mg (0.163 mmol) of **1** and 100 mg (0.180 mmol) of NiXantphos in benzene for two hours followed by column chromatography separation gave 57.8 mg (43%) of **4**. ESR (toluene-CH<sub>2</sub>Cl<sub>2</sub>, 150 K):  $g_1 = 2.524$ ,  $g_2 = 2.043$ ,  $g_3 = 1.937$ ; IR (KBr): 2563 cm<sup>-1</sup> ( $\nu$ (B-H)). MALDI MS ( $M^-$ , max): 820.3 ( $M^-$ ; isotopic pattern for 1Ru, 1Cl, 9B atoms), calcd.: 820.2.

[3,3- $\kappa^2$ -Xantphos-3-NCCH<sub>3</sub>-closo-3,1,2-RuC<sub>2</sub>B<sub>9</sub>H<sub>11</sub>] (**3**) Complex **2** (24 mg, 0.028 mmol) was placed in a Schenk tube followed by 2 mL of CH<sub>2</sub>Cl<sub>2</sub>, 2 mL of CH<sub>3</sub>CN and 0.12 mL (1.4 mmol) of isopropylamine. The tube was degassed via three freeze-pump-thaw cycles and filled with argon. The reaction was conducted at room temperature under stirring for 2.5 h. The solution was placed on a silica-gel filled column and a bright-yellow band was eluted with acetonitrile-ethyl acetate (1:1) mixture. The solvent was evaporated. Recrystallization of a residue from hot acetonitrile gave 10.5 mg (44%) of complex **3**. <sup>1</sup>H NMR (CD<sub>2</sub>Cl<sub>2</sub>, 400 MHz):  $\delta$  6.73–7.62 (26H, m, Ph+Xantphos), 2.83 (2H, br, C<sub>carb</sub>H), 2.47 + 1.69 (3H + 3H, s, CH<sub>3</sub>); 1.97 (3H, s, CH<sub>3</sub>-CN). <sup>31</sup>P{<sup>1</sup>H} NMR (CD<sub>2</sub>Cl<sub>2</sub>, 162 MHz),  $\delta$ : 35.21 (s) ppm. <sup>11</sup>B{<sup>1</sup>H} NMR (CD<sub>2</sub>Cl<sub>2</sub>, 128 MHz):  $\delta$ : -25.3 (1B), -11.2 (3B), -7.69 (2B), -5.72 (2B), -0.43 (1B). IR (KBr): 2254 cm<sup>-1</sup> ( $\nu$ (C≡N)). MALDI MS ( $M^+$ , max): 812.3 ([M-CH<sup>3</sup>CN]<sup>+</sup>; isotopic pattern for 1Ru, 9B atoms), calcd.: 812.2.

[3,3- $\kappa^2$ -NiXantphos-3-NCCH<sub>3</sub>-closo-3,1,2-RuC<sub>2</sub>B<sub>9</sub>H<sub>11</sub>] (**5**) The procedure is similar as for the complex **3**. The reaction of 25 mg (0.030 mmol) of **4** with 0.12 mL (1.4 mmol) of isopropylamine in the mixture of 2 mL of acetonitrile and 2 mL of CH<sub>2</sub>Cl<sub>2</sub> followed by column chromatography separation gave 18.3 mg (73%) of **5**. <sup>1</sup>H NMR (CD<sub>2</sub>Cl<sub>2</sub>, 400 MHz):  $\delta$  8.1 (1H, br, NH), 6.6–7.6 (26H, m, Ph+NiXantphos), 2.98 (2H, br, C<sub>carb</sub>H), 1.97 (3H, s, CH<sub>3</sub>-CN). <sup>31</sup>P{<sup>1</sup>H} NMR (CD<sub>2</sub>Cl<sub>2</sub>, 162 MHz),  $\delta$ : 29.25 (s) ppm. <sup>1</sup>IR (KBr): 2245 cm<sup>-1</sup> ( $\nu$ (C≡N)), 2553 cm<sup>-1</sup> ( $\nu$ (B-H)). MALDI MS ( $M^+$ , max): 785.2 ([M-CH<sub>3</sub>CN]<sup>+</sup>; isotopic pattern for 1Ru, 9B atoms), calcd.: 785.2.

[3,3- $\kappa^2$ -DPEphos-3-Cl-closo-3,1,2-RuC<sub>2</sub>B<sub>9</sub>H<sub>11</sub>] (**7**) The procedure is similar as for the complex **2**. Heating of 110 mg (0.138 mmol) of **6** and 104 mg (0.193 mmol) of DPEphos in benzene for 1.5 h followed by column chromatography separation gave 73.9 mg (66%) of **7**. ESR (toluene-CH<sub>2</sub>Cl<sub>2</sub>, 150 K):  $g_1 = 2.433$ ,  $g_2 = 2.068$ ,  $g_3 = 1.955$ ; IR (KBr): 2569 cm<sup>-1</sup> ( $\nu$ (B-H)). MALDI MS ( $M^-$ , max): 791.1 ( $M^-$ ; isotopic pattern for 1Ru, 1Cl, 9B atoms), calcd.: 791.2.

[3,3- $\kappa^2$ -DPEphos-3-NCCH<sub>3</sub>-closo-3,1,2-RuC<sub>2</sub>B<sub>9</sub>H<sub>11</sub>] (**8**) The procedure is similar as for the complex **3**. The reaction of 25 mg (0.030 mmol) of **7** with 0.12 mL (1.4 mmol) of isopropylamine in the mixture of 2 mL of acetonitrile and 2 mL of CH<sub>2</sub>Cl<sub>2</sub> followed by column chromatography separation gave 20.1 mg (80%) of **8**. <sup>1</sup>H NMR (CD<sub>2</sub>Cl<sub>2</sub>, 400 MHz):  $\delta$  6.8–7.4 (28H, m, Ph+DPEphos), 2.43 (2H, br, C<sub>carb</sub>H), 1.99 (3H, s, CH<sub>3</sub>-CN). <sup>31</sup>P{<sup>1</sup>H} NMR (CD<sub>2</sub>Cl<sub>2</sub>, 162 MHz),  $\delta$ : 24.83 (s) ppm. <sup>11</sup>B{<sup>1</sup>H} NMR (CD<sub>2</sub>Cl<sub>2</sub>, 128 MHz):  $\delta$ : -24.6 (1 B), -11.1 (3 B), -6.6 (2 B), -5.2 (2 B), -0.18 (1 B). IR (KBr): 2276 cm<sup>-1</sup> ( $\nu$ (C≡N)), 2538 cm<sup>-1</sup> ( $\nu$ (B-H)). MALDI MS ( $M^+$ , max): 756.3 ([M-CH<sub>3</sub>CN]<sup>+</sup>; isotopic pattern for 1Ru, 9B atoms), calcd.: 756.2.

*An one-step synthesis of complexes 3, 5 and 8 from 1.* 141 mg (0.177 mmol) of **1** were placed in a Schlenk tube followed by 4 mL of acetonitrile and 0.25 mL (1.8 mmol) of triethylamine. The tube was degassed via three freeze-pump-thaw cycles and filled with argon. The reaction mixture was stirred at room temperature for 10 min and 105 mg (0.195 mmol) of DPEphos were added in argon flush. The reaction mixture was stirred at room temperature for 24 h giving yellow precipitate. The latter was washed by n-hexane and dried in vacuum giving 106.3 mg (74%) of yellow product. The NMR and MALDI spectra are similar to the

same of **8**. In a similar way starting from 50 mg (0.062 mmol) of **1** and 0.27 mL (2.5 mmol) of isopropylamine and 38.2 mg (0.069 mmol) of NiXantphos 42 mg (80.7%) of **5** were received. Starting from 30 mg (0.037 mmol) of **1** and 0.16 mL (1.5 mmol) of isopropylamine and 24 mg (0.041 mmol) of Xantphos 16.5 mg (50.6%) of **5** were received.

### 3.3. X-ray Diffraction Study

The X-ray single-crystal data were collected using Mo K $\alpha$  radiation ( $\lambda = 0.71073 \text{ \AA}$ ) on an Oxford Diffraction Gemini S diffractometer. The crystallographic parameters and the X-ray-data-collection and structure-refinement statistics are given in Table 5. The primary structure was solved by structure-invariant direct methods using SHELX [24] and WinGX [25]. The positions of other atoms were determined by the difference syntheses of electron density and were refined against  $|F|^2$  by the least squares method. Hydrogen atoms were placed in geometrically calculated positions which were refined according to the riding model. The crystallographic data have been deposited in the Cambridge Crystallographic Data Centre under the deposition codes CCDC 2165075 (2), 2165074 (3), 2165064 (5) and 2214909 (9).

**Table 5.** The crystal data, data collection and structure refinement parameters for ruthenacarboranes **2**, **3**, **5**.

Compound	2	3	5	9
CCDC No	2165075	2165074	2165064	2214909
Empirical formula	C <sub>41</sub> H <sub>43</sub> B <sub>9</sub> ClOP <sub>2</sub> Ru 2 C <sub>6</sub> H <sub>6</sub>	C <sub>43</sub> H <sub>46</sub> B <sub>9</sub> NOP <sub>2</sub> Ru 2 CH <sub>2</sub> Cl <sub>2</sub>	C <sub>40</sub> H <sub>41</sub> B <sub>9</sub> N <sub>2</sub> P <sub>2</sub> Ru CH <sub>3</sub> CN	C <sub>38.75</sub> H <sub>40.50</sub> B <sub>9</sub> Cl <sub>1.50</sub> O <sub>3</sub> P <sub>2</sub> Ru
Molecular weight	1003.72	1022.96	867.1	867.68
Crystal size (mm)	0.845 × 0.397 × 0.211	0.561 × 0.28 × 0.22	0.216 × 0.112 × 0.092	0.342 × 0.222 × 0.062
Temperature (K)	297(2)	293(2)	100(2)	100(2)
Crystal system	Monoclinic	Triclinic	Triclinic	Monoclinic
Space group	P2 <sub>1</sub> /c	P $\bar{1}$	P $\bar{1}$	P2 <sub>1</sub> /c
a (Å)	12.2652(2)	11.3175(4)	11.6015(14)	12.9051(4)
b (Å)	22.0922(2)	11.6877(4)	12.9626(16)	17.3631(2)
c (Å)	22.7267(4)	18.8933(6)	15.7089(15)	23.3119(7)
$\beta$ (deg)	125.048(3)	83.161(3)	93.373(9)	129.448(5)
V (Å <sup>3</sup> )	5041.5(2)	2468.62(15)	2119.4(5)	4033.6(3)
Z	4	2	2	4
D <sub>calcd</sub> (g.cm <sup>-3</sup> )	1.322	1.376	1.359	1.429
linear absorption $\mu$ (cm <sup>-1</sup> )	4.66	6.35	4.83	6.05
T <sub>min</sub> /T <sub>max</sub>	0.801/0.925	0.809/0.913	0.599/1	0.92212/1
Reflections collected	105,544	39,245	14,935	105,579
Independent reflections (R <sub>int</sub> )	15,316 (0.0373)	12,224 (0.031)	8323 (0.052)	8224
Observed reflections (I > 2 $\sigma$ (I))	12,773	10,834	5852	7511
Number of parameters	765	571	525	515
R <sub>1</sub> (on F for I > 2 $\sigma$ (I))	0.052	0.0435	0.1179	0.0377
wR <sub>2</sub> (on F <sup>2</sup> for all data)	0.1343	0.1263	0.2995	0.0930
GOOF	1.147	1.04	1.259	1.057
Largest diff. peak/hole (e Å <sup>-3</sup> )	0.922/−0.637	0.821/−0.958	3.376/−1.702	1.573/−0.848

### 3.4. Quantum-Chemical Calculations

The geometry calculations for the ruthenacarboranes were carried out using the Gaussian 03 suite of programs [26] in terms of the density functional theory. For all optimized geometries, the vibrational frequencies were calculated. The calculations were performed with the use of the B3PW91 functional [27] and a composite basis set consisting of 6-31G(d) basis functions for elements of Periods 1–3 and the Lanl2DZ basis set [28], which includes the effective pseudopotential (ECP) modeling the behavior of the core electrons, for the ruthenium atom. The QST3 method was used to determine geometries of the transition states.

### 3.5. Polymerization Procedure

To avoid the error with dosage of small initiator quantities and a 0.1 M CCl<sub>4</sub> solution in toluene was prepared. The predetermined amount of ruthenium complex (0.0047 mmol) was dissolved in 1.18 mL (0.118 mmol) of 0.1 M CCl<sub>4</sub> solution in a round-bottom flask. After full dissolution of 15.4 μL (0.188 mmol) of *i*-PrNH<sub>2</sub> and 5 mL (47 mmol) of MMA were added. The resulting mixture was poured out into five glass tubes (ca. 1.2 mL into each, the tubes were weighted before and after addition of the mixture) and the reaction mixture was degassed via three freeze-pump-thaw cycles to remove oxygen. The tubes were set to a thermostat for a certain time. The polymerization was stopped by freezing the tube with the reaction mixture by liquid nitrogen. The resulting polymer was precipitated into excess of *n*-hexane. In order to purify the polymers from residual amounts of the monomer, initiator, and the metallocarborane catalyst, the samples were twice dissolved in dichloromethane and precipitated into *n*-hexane. After second precipitation the samples were dried in vacuum to a constant weight.

## 4. Conclusions

Thus we may conclude that Xantphos, NiXantphos and DPEphos may be used as chelate ligands for formation of *closo*-ruthenacarborane complexes of ruthenium (II) and (III). The structure, reactivity and redox properties of the formed compounds is generally similar to the relative complexes with bis(diphenylphosphino)alkanes. The first two diphosphines containing rigid condensed aromatic fragment act only as a κ<sup>2</sup>-ligands, occupying two adjacent coordination sites at ruthenium center. The flexibility of DPEphos ligand results in additional intermolecular interaction between ruthenium and oxygen atoms leading to the formation of labile facial κ<sup>3</sup>-coordinated complex which formation was confirmed by NMR spectrometry. The shielding of the ruthenium center in 16-e species results in the loss of catalytic activity of DPEphos-based complexes in ATRP process as it was earlier observed for κ<sup>3</sup>-complexes with chelate triphosphines [29].

**Supplementary Materials:** The following supporting information can be downloaded at: <https://www.mdpi.com/article/10.3390/inorganics10110206/s1>, Figure S1. Anisotropic EPR spectra of ruthenacarboranes 2, 4 and 7 in toluene-CH<sub>2</sub>Cl<sub>2</sub> matrix at 150 K; Figure S2. <sup>1</sup>H NMR spectrum of complex 3. Solvent—CD<sub>2</sub>Cl<sub>2</sub>; Figure S3. <sup>11</sup>B{<sup>1</sup>H} NMR spectrum of complex 3. Solvent—CD<sub>2</sub>Cl<sub>2</sub>; Figure S4. <sup>1</sup>H NMR spectrum of complex 5. Solvent—CD<sub>2</sub>Cl<sub>2</sub>; Figure S5. <sup>1</sup>H NMR spectrum of complex 8. Solvent—CD<sub>2</sub>Cl<sub>2</sub>; Figure S6. <sup>11</sup>B{<sup>1</sup>H} NMR spectrum of complex 8. Solvent—CD<sub>2</sub>Cl<sub>2</sub>.

**Author Contributions:** Synthesis of metallocarboranes, HPLC experiments and manuscript writing, A.M.Z.; single crystal X-ray diffraction experiments N.V.S., NMR spectroscopy, Y.B.M.; polymerization experiments, N.A.K.; EPR study, A.V.P.; manuscript concept, electrochemical and MALDI MS experiments, quantum-chemical calculations, supervision, and manuscript writing, I.D.G. All authors have read and agreed to the published version of the manuscript.

**Funding:** The work was supported by the Grant of President of Russian Federation (proj. No. MD-1474.2022.1.3).

**Data Availability Statement:** Crystallographic data for the structures of compounds 2, 3, 5 and 9 were deposited with the Cambridge Crystallographic Data Centre as supplementary publications CCDC 2165064, 2165074, 21650754 and 2214909. The Supplementary Information contains NMR spectra of compounds 3, 5 and 8, ESR spectra of compounds 2, 4 and 7.

**Acknowledgments:** The study was carried out on the equipment of the Collective Usage Center “New Materials and Resource-saving Technologies” of Lobachevsky State University of Nizhny Novgorod.

**Conflicts of Interest:** The authors declare no conflict of interest.

## References

1. Lorandi, F.; Matyjaszewski, K. Why do we need more active ATRP catalysts? *Isr. J. Chem.* **2019**, *60*, 108–123. [CrossRef]
2. Bultz, E.; Ouchi, M.; Sawamoto, M.; Cunningham, M.F. “Smart” catalysis with thermoresponsive ruthenium catalysts for miniemulsion Ru-mediated reversible deactivation radical polymerization cocatalyzed by smart iron cocatalysts. *J. Polym. Sci. A Polym. Chem.* **2019**, *57*, 305–312. [CrossRef]

3. Grishin, I.D.; Zimina, A.M.; Anufriev, S.A.; Knyazeva, N.A.; Piskunov, A.V.; Dolgushin, F.M.; Sivaev, I.B. Synthesis and Catalytic Properties of Novel Ruthenacarboranes Based on nido-[5-Me-7,8-C<sub>2</sub>B<sub>9</sub>H<sub>10</sub>]<sup>2-</sup> and nido-[5,6-Me<sub>2</sub>-7,8-C<sub>2</sub>B<sub>9</sub>H<sub>9</sub>]<sup>2-</sup> Dicarbollide Ligands. *Catalysts* **2021**, *11*, 1409. [[CrossRef](#)]
4. Zimina, A.M.; Knyazeva, N.A.; Balagurova, E.V.; Dolgushin, F.M.; Somov, N.V.; Vorozhtsov, D.L.; Malysheva, Y.B.; Grishin, I.D. Revising the chemistry of  $\kappa^2$ -dppe-closo-RuC<sub>2</sub>B<sub>9</sub>H<sub>11</sub> fragment: Synthesis of novel diamagnetic complexes and its transformations. *J. Organomet. Chem.* **2021**, *946–947*, 121908. [[CrossRef](#)]
5. Penkal, A.M.; Somov, N.V.; Shchegravina, E.S.; Grishin, I.D. Ruthenium Diphosphine Closo-C<sub>2</sub>B<sub>9</sub>-Carborane Clusters with Nitrile Ligands: Synthesis and Structure Determination. *J. Clust. Sci.* **2019**, *30*, 1317–1325. [[CrossRef](#)]
6. Penkal, A.M.; D'yachihin, D.I.; Somov, N.V.; Shchegravina, E.S.; Grishin, I.D. Synthesis of novel closo-carborane complexes of ruthenium (II) with triphenylphosphine or acetonitrile ligands via reduction of paramagnetic Ru(III) derivatives. *J. Organomet. Chem.* **2018**, *872*, 63–72. [[CrossRef](#)]
7. D'yachikhin, D.I.; Grishin, I.D.; Dolgushin, F.M.; Godovikov, I.A.; Chizhevsky, I.T.; Grishin, D.F. Synthesis, isomerism, and catalytic properties of chelate ruthenium copper bimetallic carborane cluster exo-closo-(Ph<sub>3</sub>P)Cu(μ-H)Ru[Ph<sub>2</sub>P(CH<sub>2</sub>)<sub>4</sub>PPh<sub>2</sub>](η<sup>5</sup>-C<sub>2</sub>B<sub>9</sub>H<sub>11</sub>), in radical polymerization of methyl methacrylate. *Russ. Chem. Bull.* **2010**, *59*, 1145–1151. [[CrossRef](#)]
8. Higashi, S.; Takenaka, H.; Ito, Y.; Oe, Y.; Ohta, T. Synthesis of RuCl<sub>2</sub>(xantphos)L (L = PPh<sub>3</sub>, P(OPh)<sub>3</sub>, DMSO) Complexes, and their Catalytic Activity for the Addition of Carboxylic Acids onto Olefins. *J. Organomet. Chem.* **2015**, *791*, 46–50. [[CrossRef](#)]
9. Adams, G.M.; Weller, A.S. POP-type ligands: Variable coordination and hemilabile behaviour. *Coord. Chem. Rev.* **2018**, *355*, 150–172. [[CrossRef](#)]
10. Takahashi, K.; Yamashita, M.; Nozaki, K. Tandem Hydroformylation/Hydrogenation of Alkenes to Normal Alcohols Using Rh/Ru Dual Catalyst or Ru Single Component Catalyst. *J. Am. Chem. Soc.* **2012**, *134*, 18746–18757. [[CrossRef](#)]
11. Venkateswaran, R.; Mague, J.T.; Balakrishna, M.S. Ruthenium(II) Complexes Containing Bis(2-(diphenylphosphino)phenyl) Ether and Their Catalytic Activity in Hydrogenation Reactions. *Inorg. Chem.* **2007**, *46*, 809–817. [[CrossRef](#)] [[PubMed](#)]
12. Deb, B.; Borah, B.J.; Sarmah, B.J.; Das, B.; Dutta, D.K. Dicarboxylruthenium(II) complexes of diphosphine ligands and their catalytic activity. *Inorg. Chem. Commun* **2009**, *12*, 868–871. [[CrossRef](#)]
13. Grishin, I.D.; D'yachihin, D.I.; Piskunov, A.V.; Dolgushin, F.M.; Smolyakov, A.F.; Il'in, M.M.; Davankov, V.A.; Chizhevsky, I.T.; Grishin, D.F. Carborane complexes of ruthenium(III): Studies on thermal reaction chemistry and the catalyst design for atom transfer radical polymerization of methyl methacrylate. *Inorg. Chem.* **2011**, *50*, 7574–7585. [[CrossRef](#)] [[PubMed](#)]
14. Grishin, I.D.; D'yachihin, D.I.; Turmina, E.S.; Dolgushin, F.M.; Smol'yakov, A.F.; Piskunov, A.V.; Chizhevsky, I.T.; Grishin, D.F. Mononuclear closo-ruthenacarborane complexes containing a rare eight-membered metal-diphosphine ring. *J. Organomet. Chem.* **2012**, *721–722*, 113–118. [[CrossRef](#)]
15. Jones, J.J.; English, L.E.; Robertson, A.P.M.; Rosair, G.M.; Welch, A.J. Mixed-ligand (triphenylphosphine)ruthenium complexes of diphenylcarborane by ligand manipulation and an asymmetric, bimolecular “symbiotic” cluster. *J. Organomet. Chem.* **2018**, *865*, 65–71. [[CrossRef](#)]
16. Stogniy, M.Y.; Erokhina, S.A.; Suponitsky, K.Y.; Markov, V.Y.; Sivaev, I.B. Synthesis and crystal structures of nickel(II) and palladium(II) complexes with o-carboranyl amidine ligands. *Dalton Trans.* **2021**, *50*, 4967–4975. [[CrossRef](#)]
17. Tutusaus, O.; Vinas, C.; Nunez, R.; Teixidor, F.; Demonceau, A.; Delfosse, S.; Noels, A.F.; Mata, I.; Molins, E. The modulating possibilities of dicarbollide clusters: optimizing the Kharasch catalysts. *J. Am. Chem. Soc.* **2003**, *125*, 11830–11831. [[CrossRef](#)]
18. Teixeira, R.G.; Marques, F.; Robalo, M.P.; Fontrodona, X.; Garcia, M.H.; Crich, G.S.; Vinas, C.; Valente, A. Ruthenium carboranyl complexes with 2,2'-bipyridine derivatives for potential bimodal therapy application. *RSC Adv.* **2020**, *10*, 16266–16276. [[CrossRef](#)]
19. Van der Veen, L.A.; Keeven, P.H.; Schoemaker, G.C.; Reek, J.N.H.; Kamer, P.C.J.; van Leeuwen, P.W.N.M.; Lutz, M.; Spek, A.L. Origin of the Bite Angle Effect on Rhodium Diphosphine Catalyzed Hydroformylation. *Organometallics* **2000**, *19*, 872–883. [[CrossRef](#)]
20. Kostukovich, A.Y.; D'yachihin, D.I.; Dolgushin, F.M.; Smol'yakov, A.F.; Godovikov, I.A.; Chizhevsky, I.T. An Unusual Conversion of Paramagnetic [3-Cl-3,3,8-{Ph<sub>2</sub>P(CH<sub>2</sub>)<sub>n</sub>PPh-μ-(C<sub>6</sub>H<sub>4</sub>-ortho)}-1,2-(CH<sub>3</sub>)<sub>2</sub>-closo-3,1,2-Ru<sup>III</sup>C<sub>2</sub>B<sub>9</sub>H<sub>8</sub>] (n = 3 and 4) to Form the First 18-Electron P-Phenylene ortho-Cycloboronated closo-Ruthenacarboranes with a Dioxygen Ligand. *Molecules* **2014**, *19*, 7094–7103. [[CrossRef](#)]
21. Kirchner, K.; Mauthner, K.; Mereiter, K.; Schmid, R. Irreversible binding of dioxygen and other gases to a half-sandwich ruthenium(II) complex: X-ray structure of [Ru(η<sup>2</sup>-O<sub>2</sub>)(η<sup>5</sup>-C<sub>5</sub>Me<sub>5</sub>)(Ph<sub>2</sub>PCH<sub>2</sub>CH<sub>2</sub>PPh<sub>2</sub>)]PF<sub>6</sub>. *J. Chem. Soc. Chem. Commun.* **1993**, *11*, 892–894. [[CrossRef](#)]
22. Chizhevsky, I.T.; Lobanova, I.A.; Bregadze, V.I.; Petrovskii, P.V.; Antonovich, V.A.; Polyakov, A.V.; Yanovsky, A.I.; Struchkov, Y.T. The first exo-nido-ruthenacarborane clusters. Synthesis and molecular structure of 5,6,10-[Cl(PPh<sub>3</sub>)<sub>2</sub>Ru]-5,6,10-μ-(H)<sub>3</sub>-10-H-7,8-C<sub>2</sub>B<sub>9</sub>H<sub>11</sub>. *Mendeleev. Commun.* **1991**, *1*, 47–49. [[CrossRef](#)]
23. Cheredilin, D.N.; Balagurova, E.V.; Godovikov, I.A.; Solodovnikov, S.P.; Chizhevsky, I.T. Facile formation of exo-nido→closo-rearrangement products upon the replacement of PPh<sub>3</sub> ligands with bis(diphenylphosphino)alkanes in “three-bridge” ruthenacarborane 5,6,10-[RuCl(PPh<sub>3</sub>)<sub>2</sub>]-5,6,10-(μ-H)<sub>3</sub>-10-H-exo-nido-7,8-C<sub>2</sub>B<sub>9</sub>H<sub>8</sub>. *Russ. Chem. Bull.* **2005**, *54*, 2535–2539. [[CrossRef](#)]
24. Sheldrick, G.M. SHELXT—Integrated space-group and crystal structure determination. *Acta Crystallogr. Sect. A* **2015**, *71*, 3–8. [[CrossRef](#)]
25. Farrugia, L.J. WinGX suite for small molecule single-crystal crystallography. *J. Appl. Crystallogr.* **1999**, *32*, 837–838. [[CrossRef](#)]

26. Frisch, M.J.; Trucks, G.W.; Schlegel, H.B.; Scuseria, G.E.; Robb, M.A.; Cheeseman, J.R.; Montgomery, J.A., Jr.; Vreven, T.; Kudin, K.N.; Burant, J.C.; et al. *Pople, Gaussian 03, Revision E.01*; Gaussian, Inc.: Wallingford, CT, USA, 2004.
27. Perdew, J.P.; Wang, Y. Accurate and simple analytic representation of the electron-gas correlation energy. *Phys. Rev. B.* **1992**, *45*, 13244–13249. [[CrossRef](#)]
28. Hay, P.J.; Wadt, W.R. Ab initio effective core potentials for molecular calculations. Potentials for the transition metal atoms Sc to Hg. *J. Chem. Phys.* **1985**, *82*, 270–283. [[CrossRef](#)]
29. Kaltenberg, A.A.; Somov, N.V.; Malysheva, Y.B.; Knyazeva, N.A.; Piskunov, A.V.; Grishin, I.D. Novel carborane complexes of ruthenium with tridentate phosphine ligands: Synthesis and application in Atom Transfer Radical Polymerization. *J. Organomet. Chem.* **2020**, *917*, 121291. [[CrossRef](#)]